2013 IEEE/RSJ International Conference on
Intelligent Robots and Systems (IROS)
November 3-7, 2013. Tokyo, Japan

A Modified Impedance Control for Physical Interaction of UAVs

Matteo Fumagalli and Raffaella Carloni

Abstract— **This paper proposes a modified impedance control strategy for a generic robotic system that can interact with an unknown environment or can be moved by a human. The controller makes use of a virtual mass, coupled to the robotic system, which allows for stable interaction. The focus is mainly on unmanned aerial vehicles that are required to get into contact with the environment to perform a specific task on it and that can be shifted by humans. The control architecture is validated both in simulations, on a 1-dimensional benchmark, and in experiments on a real quadrotor flying vehicle.**

I. INTRODUCTION

Current trends in robotics foster research in development of capabilities and skills that can make robots autonomous and safe. The evolving scenario requires the human and the robot to coexist within a shared environment, to interact and to safely perform both independent and cooperative tasks.

Among the latest research developments, which are focusing on physical interaction, the control of unmanned aerial vehicles (UAVs) is one of the most promising research category due to the width of its application spectrum.

Unmanned aerial vehicles have the intrinsic characteristics of being floating base robotic systems [1]. Limiting the treatment to miniature rotorcrafts, UAVs represent a class of robots with ideally unbounded workspace and that can be extremely versatile for performing tasks both autonomously and in cooperation with humans. Transportation [2], inspection [3], structure assembly [4] are application scenarios for the research on UAVs interaction control. UAVs have been successfully exploited in object grasping and transportation [4], [5], wall painting [6], wall inspection [7], [8].

Although typically considered as dexterous systems, UAV rotorcraft are typically characterized by being under-actuated vehicles. This means that, due to the lack of actuators along certain directions, the system has to combine the motion of its actuated degrees of freedom in order to perform a trajectory along the non actuated ones. More specifically, when a rotorcraft UAV, e.g. a quadrotor, is required to move along a lateral direction, the platform should tilt in order to generate the necessary command force to achieve the task.

The control of this type of system is typically achieved by a cascade of controllers, where a position or impedance control loop is closed on top of a high gains attitude controller [7]. Due to the nature of this type of control system, when an interaction occurs, it is not guaranteed that the internal dynamics remains stable.

This paper proposes a modified impedance control for a generic robotic system and, specifically, for a quadrotor UAV. The controller exploits a *virtual mass*, according to which the UAV can dynamically adapt during the interaction with a remote environment while preserving stability. The advantage of controlling this behavior is that, given an externally applied interaction force, the UAV behaves as an unconstrained impedance. More precisely, two scenarios are foreseen. First, while the UAV is moving, it can get into contact with the environment and stabilize on it. Second, if the vehicle is hovering and a human pushes it by applying a force, the UAV moves away till it finds a new equilibrium position further from the human.

The paper is organized as follows. Section II gives an overview of the proposed control strategy for a generic robotic system. Section III shows the simulation of the control law on a simplified mono-dimensional system. The case of a quadrotor UAV is described in Section IV, where experimental results are validating the proposed control law. Finally, concluding remarks are drawn in Section V.

II. CONTROL

This section presents the proposed method as a general approach to robotic interaction control, and is applied to the case of a quadrotor UAV in section Section IV.

Robotic systems interacting in an unstructured environment are generally controlled in such way that they show a certain compliance when external forces are applied. Sensorless control scheme are generally preferable to control architectures in which a force sensor is used as a direct feedback. Impedance controlled systems are typically used in interaction control to guarantee a certain level of compliance of the robotic system by controlling the relation between force and position (velocity). A typical implementation is represented by assigning to the system the behavior of a mass-spring-damper system, as sketched in Figure 1. Nevertheless, the lack of force sensors do not allow to properly monitor the interaction force.

The control scheme proposed in this work allows to qualitatively control the interaction arising between the robotic system and an unknown environment due to contacts, without requiring the use of force measurements. The controller exploits the dynamics of an additional virtual dynamical system, i.e. a virtual mass, to monitor the interaction of the real system, and eventually control it by means of a force input to the virtual system.

This work has been partially funded by the European Commission's Seventh Framework Programme as part of the project AIRobots under grant no. 248669.

M. Fumagalli and R. Carloni are with the Faculty of Electrical Engineering, Mathematics and Computer Science, University of Twente, The Netherlands. Email: {m.fumagalli, r.carloni}@utwente.nl

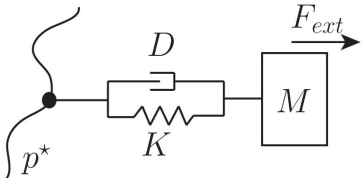

Fig. 1. Schematic representation of an equivalent impedance controlled system.

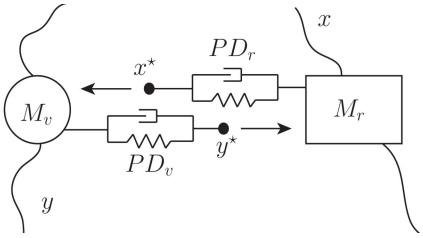

Fig. 2. Schematic representation of the proposed control scheme.

A. The Low Level Controller

Let consider a generic system of the form:

$$M_r(x)\ddot{x} + C(x,\dot{x}) + G(x) = \tau - J^\top F_{ext} \tag{1}$$

where $x \in \mathbb{R}^n$ is the position vector of the system, $M_r(x) \in \mathbb{R}^{n\times n}$ the inertia matrix, $C \in \mathbb{R}^n$ the Coriolis and centrifugal terms, $G \in \mathbb{R}^n$ the gravitational component, $\tau \in \mathbb{R}^n$ the actuation torque, $J \in \mathbb{R}^{n\times 6}$ the system geometric Jacobian and $F_{ext} \in \mathbb{R}^6$ the external wrench.

Moreover, let define τ in such a way that it ideally cancels the nonlinear terms of the dynamics of the system. It follows that the system takes the form:

$$\ddot{x} = u - \hat{f}_{ext} \tag{2}$$

being u a new control input to the system and $\hat{f}_{ext} := M_r(x)^{-1} f_{ext}$, in which $f_{ext} := J^\top F_{ext}$. If we define u to take the form:

$$u = -\hat{D}_r\dot{\tilde{x}} - \hat{K}_r\tilde{x} \tag{3}$$

where $\tilde{x} = x - x^\star$ is the position error, $x^\star$ is the reference position of the new controlled system, and where we define $\hat{D}_r = M_r(x)^{-1}D_r$ and $\hat{K}_r = M_r(x)^{-1}K_r$ as the desired damping and stiffness matrices, then the overall dynamics takes the form:

$$M_r(x)\ddot{x} + D_r\dot{\tilde{x}} + K_r\tilde{x} = f_{ext} \tag{4}$$

The resulting controlled systems shows a behavior that is characterized by a second order dynamical system, whose reference position $x^\star$ can be chosen arbitrarily, thus being a novel control input to the plant.

B. The Virtual Mass Controller

The proposed modified impedance controller is build for the system described by (4). It exploits a virtual dynamical system to dynamically modify the position reference $x^\star$ to the real system (4) in such a way that, when the real system undergoes an interaction, the virtual system can be used to monitor the interaction forces and possibly to modify them. To obtain this, let M_v be a virtual mass subject to the virtual input ψ, i.e.:

$$M_v\ddot{y} = \psi \tag{5}$$

where $M_v \in \mathbb{R}^{n\times n}$ is the mass matrix of the virtual system and $\psi \in \mathbb{R}^n$ the control input to the virtual system. Let the control input ψ be of the form:

$$\psi = -D_v\dot{\tilde{y}} - K_v\tilde{y} + \hat{f}_v \tag{6}$$

where $\tilde{y} = y - y^\star \in \mathbb{R}^n$ is the distance vector between the desired position $y^\star \in \mathbb{R}^n$ and the actual position of the virtual mass, $D_v \in \mathbb{R}^{n\times n}$ and $K_v \in \mathbb{R}^{n\times n}$ are the damping and the stiffness matrices, respectively, and $\hat{f}_v \in \mathbb{R}^n$ a new control input for the controlled virtual mass. The overall dynamics of the virtual mass thus becomes:

$$M_v\ddot{y} + D_v\dot{\tilde{y}} + K_v\tilde{y} = \hat{f}_v \tag{7}$$

The behavior of the virtual system is described by an impedance relation, characterized by a second order dynamics, as for (4), where the reference trajectory is given by $y^\star$ and $\dot{y}^\star$, and whose control input is $\hat{f}_v$.

If we interconnect the two systems represented by (4) and (7) so that the reference position to track for the virtual system $y^\star$ becomes the actual position of the real system, i.e., $y^\star = x$, and, on the other hand, the reference position for the real system $x^\star$ becomes the actual position of the virtual system, i.e., $x^\star = y$, the overall coupled dynamics becomes:

$$\begin{cases} M_r\ddot{x} + D_r\left(\dot{x} - \dot{y}\right) + K_r\left(x - y\right) = f_{ext} \\ M_v\ddot{y} + D_v\left(\dot{y} - \dot{x}\right) + K_v\left(y - x\right) = \hat{f}_v \end{cases} \tag{8}$$

These equations show that, since the dampings and stiffnesses describing the dynamics of the two systems are not necessarily the same, the exchanged forces are unbalanced and, therefore, the two systems are interconnected by means of an asymmetric coupling. The overall system, described by (8), can be proven to be marginally stable by choosing $\hat{f}_v = D_{v,2}\dot{y} + f_v$, where $D_{v,2}\dot{y}$ is an absolute damping force opposing the motion of the virtual system and f_v the new control input.

By introducing the virtual mass, it is possible to directly access the virtual input force f_v and, therefore, to control the real robotic system dynamics. As a matter of facts, the controlled system is perturbed, i.e., accelerated in the direction of f_v. When the system is in steady state, f_{ext} and f_v are balanced and the relative equilibrium position of the virtual and real systems is determined by the stiffnesses K_r and K_v. When the real system enters into contact with an obstacle, either a wall or a human, a force f_{ext} is generated, which can be modulated through control by selecting f_v.

Note that both the gains K_v and D_v and the mass of the virtual system M_v influence the response of the real system. The mass of the virtual system, which can be chosen arbitrarily, affects the transient of the overall controlled system: a high value of M_v, compared to M_r, causes an increase in the inertia of the overall controlled system and,

therefore, the controlled system has a slower dynamics. On the other hand, a low value of M_v makes the dynamics of the virtual mass faster. Therefore, depending on the type of application the proposed control architecture is designed for, the control parameters should be tuned accordingly. In particular, high K_v and low M_v should be chosen if the purpose is to observe the interaction force without highly influencing the dynamics of the real system.

III. SIMULATION

In this section, we evaluate the proposed control architecture on a 1-dimensional benchmark. The dynamics of the real mass m_r is given by:

$$m_r\ddot{x}_r + d_r\left(\dot{x}_r - \dot{x}_v\right) + k_r\left(x_r - x_v\right) = f_{ext} \qquad (9)$$

where x_r, $\dot{x}_r$ and $\ddot{x}_r$ are the position, velocity and acceleration, respectively; k_r and d_r are the stiffness and damping coefficients, describing the interconnection to the virtual mass; f_{ext} is the external force.

The dynamics of the virtual mass m_v is given by:

$$m_v\ddot{x}_v + d_v\left(\dot{x}_v - \dot{x}_r\right) + k_v\left(x_v - x_r\right) = \hat{f}_v \qquad (10)$$

where x_v, $\dot{x}_v$ and $\ddot{x}_v$ are the position, velocity and acceleration, respectively; k_v and d_v are the stiffness and damping coefficients, describing the interconnection to the real mass; f_v is the input force.

In state space form, the overall system dynamics is:

$$\dot{\gamma} = \begin{bmatrix} -\frac{d_r}{m_r} & \frac{d_r}{m_r} & -\frac{k_r}{m_r} & \frac{k_r}{m_r} \\ \frac{d_v}{m_v} & -\frac{d_v}{m_v} & \frac{k_v}{m_v} & -\frac{k_v}{m_v} \\ 1 & 0 & 0 & 0 \\ 0 & 1 & 0 & 0 \end{bmatrix} \gamma + \begin{Bmatrix} f_{ext} \\ f_v \\ 0 \\ 0 \end{Bmatrix} \qquad (11)$$

where $\gamma = [\dot{x}_r, \dot{x}_v, x_r, x_v]^T$ is the state vector of the overall system. The aforementioned system is fully controllable and can be proven to be marginally stable by choosing $\hat{f}_v = -d_{v,2}\dot{x}_v + f_v$, being $d_{v,2}\dot{x}_v$ an absolute damping force which opposes to the motion of the virtual system and f_v a new input force.

In the simulation, we assume that the real system gets into contact with a wall located at a certain position x_w. Moreover the interaction force f_{ext} is modeled by means of a Hunt-Crossley model [9], according to which the reaction force F_n is dependent on the penetration-depth η and is given by:

$$f_{ext}(\eta) = \begin{cases} k\eta(t) + \lambda\eta(t)\dot{\eta}(t) & \eta < 0 \\ 0 & \eta \geq 0 \end{cases}$$

where λ and k are respectively the damping and stiffness coefficients while the penetration η is calculated as the distance between the mass position x_r and the equilibrium position of the wall x_w, i.e., $\eta = x_w - x_r$.

Two simulation have been carried out, by setting $x_w = 0.1$ m. The first simulation shows the effect of the modification of the parameters of the virtual mass, when the system is at steady state. More specifically, Figure 3 shows the effect of varying the parameters d_v and k_v of the virtual mass, while keeping fixed the masses m_r and m_v and the parameters d_r and k_r of the real system. In the top plot of Figure 3, the

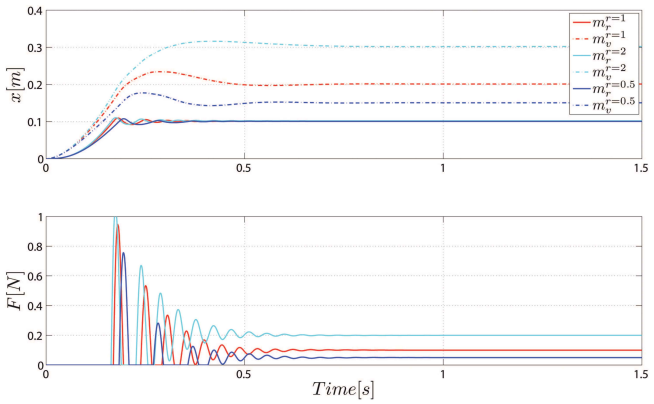

Fig. 3. Simulation results on the interaction of the virtual and real mass with the environment (m_v and m_r are constant). k_v is modified in such a way that the ratio $r = k_v/k_r$ is equal to $r = 0.5$, $r = 1$ and $r = 2$ in the three simulations. **Top**: the positions x_v (dashed lines) and x_r (continuous lines), for an applied input force f_v. At $x = 0.1$ m, the real mass motion is constrained by means of an obstacle. **Bottom**: interaction forces f_{ext} due to the interaction with the wall, for a given input force $f = 0.1$ N applied on the virtual mass.

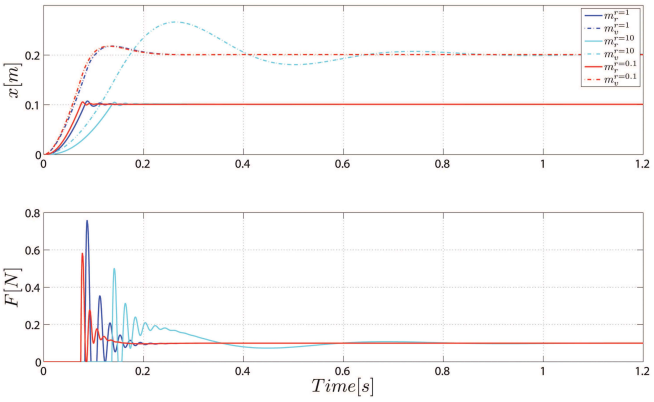

Fig. 4. Simulation results on the interaction of the virtual and real masses with the environment (k_v and m_r are constant). m_v is modified such that the ratio between the two masses $r = m_v/m_r$ is equal to $r = 0.1$, $r = 1$ and $r = 10$. **Top**: the positions x_v (dashed lines) and x_r (continuous lines), for an applied input force f_v. At $x = 0.1$ m, the real mass motion is constrained by means of an obstacle. **Bottom**: interaction forces f_{ext} due to the interaction with the obstacle, for a given input force $f = 0.1$ N applied to the virtual mass.

position of both the virtual and the real masses are reported. A constant command force f_v is applied at time $t = 0$. Around time $t = 0.2$ s, the impact of the real mass with the environment occurs. The effect on the overall system response, caused by using different proportional gains k_v and derivative gains d_v of the virtual system, is that the steady state equilibrium position of the virtual mass changes. In the bottom plot of Figure 3, the correspondent interaction forces are reported. While a constant force is continuously applied to the virtual mass ($f_v = 0.1$ N), the environment's force f_{env} exchanged between the wall and the real mass is different, depending on the gains d_v and k_v of the virtual system.

The second simulation shows the effects of the modification of the mass parameter m_v of the virtual system.

Figure 4 shows that the mass assigned to the virtual system only affects the transient of the overall controlled system and not the steady state interaction force.

IV. THE QUADROTOR UAV

The proposed control architecture have been applied to a multi-DoF non-linear system, i.e., a quadrotor UAV.

A. Dynamics of the Quadrotor

The relative thrust $f_p = [f_1\ f_2\ f_3\ f_4]^\top$ of the four propellers of a quadrotor UAV gives origin to a force f in the direction of the axis of the propellers and to the body moment $\mathbf{M}^u = [M_x\ M_y\ M_z]^T$ according to the linear relation:

$$\begin{bmatrix} f & M_x & M_y & M_z \end{bmatrix}^\top = T_M f_p \tag{12}$$

where T_M is a constant matrix which depends on the geometry of the UAV and the characteristics of the propellers. The dynamics of the quadrotor can be described by a rigid body with reference frame F_b placed in its center of gravity, which interacts with the environment at one of its side, at frame F_e. Let F_i be the inertial reference frame and let select the following notation:

- $\boldsymbol{\omega}_{\boldsymbol{r}_b}^{b,i}, \dot{\boldsymbol{\omega}}_{\boldsymbol{r}_b}^{b,i} \in \mathbb{R}^3$ are the rotational velocity and acceleration, respectively, of the UAV with respect to the inertial frame, expressed in the body-frame.
- $\mathbf{v_r}^i = \dot{p}_{r_b}^i \in \mathbb{R}^3$ and $\dot{\mathbf{v}}_\mathbf{r}{}^i = \ddot{p}_{r_b}^i \in \mathbb{R}^3$ the linear velocity and acceleration of the UAV center of gravity described in the inertial frame.
- $p_b^e \in \mathbb{R}^3$ and $R_e^b \in \mathbb{R}^{3\times3}$ the relative position and rotation matrix representing the contact frame F_e with reference to the UAV frame F_b.
- $p_i^b \in \mathbb{R}^3$ and $R_b^i \in \mathbb{R}^{3\times3}$ the relative position and rotation matrix representing the UAV frame F_b with reference to the inertial frame F_i
- $m_{uav}, J_{uav} \in \mathbb{R}$ the mass and inertial matrix of the UAV.
- $M_{gy} \in \mathbb{R}^3$ is the moment vector, which denotes the gyroscopic effects due to the rotating propellers.
- $f_{ext}^e \in \mathbb{R}^3$ and $M_{ext}^e \in \mathbb{R}^3$ are the forces and moment acting on the quadrotor at frame F_e, due to external interaction

The quadrotor dynamics is as:

$$\begin{cases} m_{uav}\dot{\mathbf{v}}_\mathbf{r}{}^i = m_{uav}g\hat{\mathbf{z}}^i + fR_b^i\,[0,0,-1]^T + \\ \qquad\qquad + R_b^i R_e^b f_{ext}^e \\ \mathbf{J_{uav}}\dot{\boldsymbol{\omega}}_b^{b,i} = -\boldsymbol{\omega}_b^{b,i} \times \mathbf{J_{uav}}\boldsymbol{\omega}_b^{b,i} + \mathbf{M}_{gy} + \mathbf{M}^u + \\ \qquad\qquad + R_b^i R_e^b M_{ext}^e + R_b^i(R_e^b f_{ext}^e \times p_e^b) \end{cases} \tag{13}$$

where it is noticeable the similarity with (1) by defining $x = \left[p_i^b, \Theta_i^b\right]^T$, where Θ_i^b is the orientation of the body frame, $\tau = \left[fR_b^{iT}\,[0,0,-1], \mathbf{M}^u\right]^T$, and the term of externally applied forces is $J^T F_{ext} = R_b^i R_e^b \left[f_{ext}^{e\top}, [M_{ext}^e + (f_{ext}^e \times p_e^b)]^\top\right]^\top$.

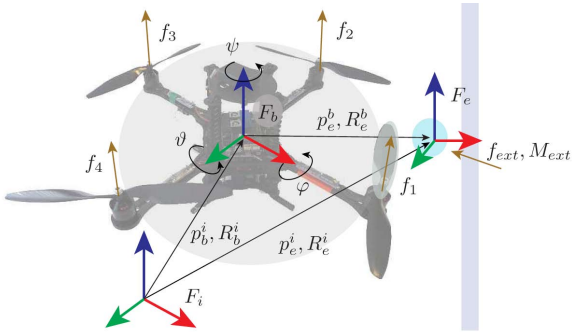

Fig. 5. Reference pictures for the description of the 3D experimental scenario. F_i indicates the inertial frame, F_b the center of gravity of the UAV, F_e the reference frame of the vehicle where interaction with the environment occurs.

B. Control

By exploiting a cascade control approach, the attitude can be controlled by means of high-gain techniques [10], to compensate for external disturbances M_{ext} and f_{ext}. In this way, the dynamic of the quadrotor can be reduced to the form of:

$$m_{uav}\dot{\mathbf{v}}_\mathbf{r}{}^i = m_{uav}g\hat{\mathbf{z}}^i + fR_b^i\,[0,0,-1]^T + R_b^i R_e^b f_{ext}^e \tag{14}$$

where the thrust force f and the attitude of the quadrotor $\Theta = [\varphi,\ \vartheta,\ \psi]^T$ become the new virtual control inputs to the system, where the latter enters into the system in the form of matrix R_b^i. The control input of the lateral and longitudinal dynamics in (14) can therefore be expressed as:

$$fR_b^i \begin{bmatrix} 0 \\ 0 \\ -1 \end{bmatrix} = \begin{bmatrix} fS_\vartheta \\ -fS_\varphi C_\vartheta \\ -fC_\varphi C_\vartheta \end{bmatrix} \tag{15}$$

where $S_\alpha = \sin(\alpha)$ and $C_\alpha = \cos(\alpha)$. The reduced dynamics of (14) does not have any dependency on the yaw angle ψ, which can therefore be considered as a separate control. The nonlinear control input of (15) can instead be considered as a function only of the thrust force f and of the components ψ and ϑ of the attitude Θ of the vehicle. In order to define an impedance behavior [11] for the quadrotor UAV to control the linear dynamics by means of the inputs f, φ and ϑ, energy-based approaches [12] in applications pertaining physical interaction between robots and the environment [13] are exploited. A graphical intuition of the overall controller for the quadrotor UAV is given in Figure 6.

By considering system (14), let the input (15) be defined as

$$f \begin{bmatrix} S_\vartheta \\ -S_\varphi C_\vartheta \\ -C_\varphi C_\vartheta \end{bmatrix} = \mathbf{u} - m_{uav}g\hat{\mathbf{z}}^i \tag{16}$$

which is well defined for all $\mathbf{u} \in \mathbb{R}^3$ such that $\left|\mathbf{u} + m_{uav}g\hat{\mathbf{z}}^i\right| > 0$, where $\mathbf{u} = [u_x,\ u_y,\ u_z]^T \in \mathbb{R}^3$ represents the vector of the new inputs. Accordingly, system

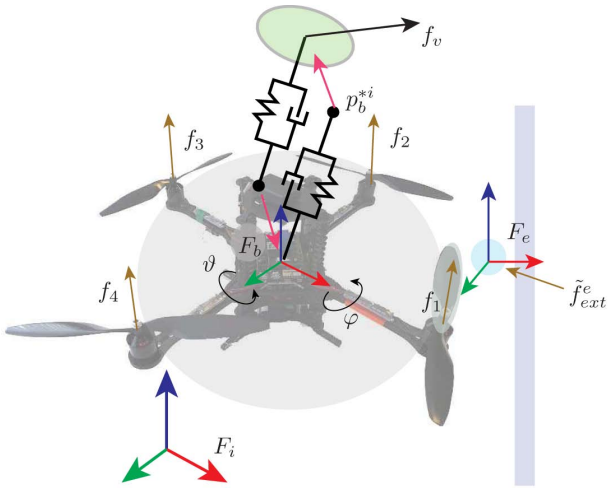

Fig. 6. Scheme of the control architecture for the quadrotor UAV.

(14) can be rewritten as

$$m_{uav}\dot{\mathbf{v}}_{\mathbf{r}}{}^i = \mathbf{u} + \tilde{f}^b_{ext} \tag{17}$$

where $\tilde{f}^b_{ext} := R^i_b R^b_m f^e_{ext}$. Let now be ${p_r}^{\star\, i}_b = [x^\star_r,\, y^\star_r,\, z^\star_r]^T$ the desired reference for the lateral, longitudinal and vertical position of the vehicle. Moreover let the control input $\mathbf{u}$ be designed as

$$\mathbf{u} = -K^r_p({p_r}^i_b - {p_r}^{\star\, i}_b) - K^r_d {\mathbf{v}_\mathbf{r}}^i \tag{18}$$

with $K^r_p, K^r_d \in \mathbb{R}^{3\times 3}$ positive definite matrices. The above linear controller can be interpreted as a passivity-based control law. In fact, observe that the resulting closed loop system is

$$m_{UAV}\dot{\mathbf{v}}_{\mathbf{r}}{}^i + K^r_d {\mathbf{v}_\mathbf{r}}^i + K^r_p({p_r}^i_b - {p_r}^{\star\, i}_b) = \tilde{f}^b_{ext} \tag{19}$$

Given the proposed controlled system, it is now possible to apply an external control loop which generates the input ${p_b}^{\star\, i}$. The additional control loop emulates the behavior of the virtual mass m_v, whose position, velocity and acceleration are described by ${p_v}^i_b$, $\mathbf{v}_v$ and $\dot{\mathbf{v}}_v$, with reference position ${p_v}^{\star\, i}_b$, stiffness K^v_p and damping K^v_d. Therefore, the overall system results governed by a dynamics which is comparable to the controlled system of (8):

$$\begin{cases} m_{UAV}\dot{\mathbf{v}}_{\mathbf{r}}{}^i + K^r_d {\mathbf{v}_\mathbf{r}}^i + K^r_p({p_r}^i_b - {p_r}^{\star\, i}_b) = \tilde{f}^b_{ext} \\ m_v \dot{\mathbf{v}}_{\mathbf{v}}{}^i + K^v_d {\mathbf{v}_\mathbf{v}}^i + K^v_p({p_v}^i_b - {p_v}^{\star\, i}_b) = f_v \end{cases} \tag{20}$$

where ${p_v}^{\star\, i}_b := {p_r}^i_b$ and ${p_r}^{\star\, i}_b := {p_v}^i_b$.

In Section IV-C, the proposed control strategy is applied to a commercial UAV, i.e. an AscTec Pelican (Ascending Technologies GmbH, Germany) quadrotor vehicle. The experiments give a qualitative evaluation of the proposed control strategy for UAV interaction. It is shown that, depending on the gains of the virtual mass, it is possible to shape the response in terms of the interaction forces, of the real vehicle interacting with a wall.

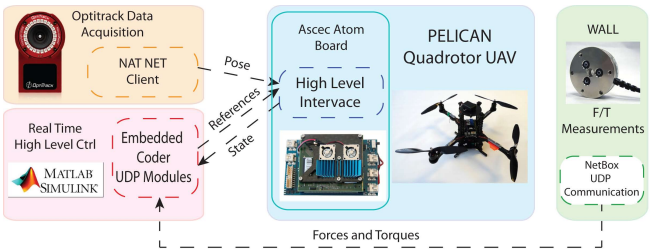

Fig. 7. The control architecture.

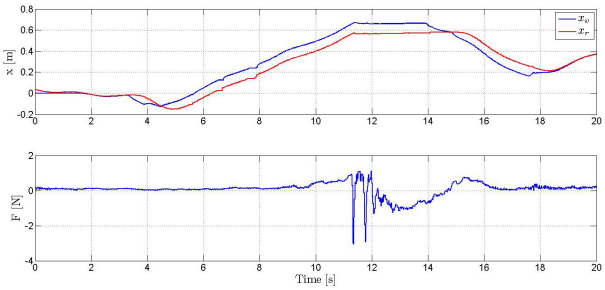

Fig. 8. The UAV is moved by means of a virtual force, applied to the virtual mass, and impacts a wall at distance $x \approx 0.55$ m. **Top**: the position of the virtual mass (blue line) and of the real mass (red line), for an applied input force on the virtual mass. At $x \approx 0.5$ m, the real mass motion is constrained by means of an obstacle. **Bottom**: interaction forces arising on the real vehicle, due to the interaction with a wall. The force on the wall in measured by an ATI-mini40E force/torque sensor.

C. Experiments

Experiments have been conducted on an Asctec Pelican quadrotor. The platform is equipped with an on-board Atom which runs the low level control of the attitude and the position control. Position is estimated using the onboard sensors (accelerometers, gyroscopes) and an external position tracking system, an OptiTrack Flex 13 (NaturalPoint, Inc., USA) based on 8 V100:R2 cameras. Optitrack data are acquired on a Windows computer and sent to the Atom board. On a second external computer, used as the ground station of the system, Matlab/Simulink (The Mathworks Inc., USA) is exploited to perform real time high level control of the vehicle, by means of the Embedded Coder toolbox.

The communication between computers is based on UDP protocol and the main communication flow is schematically represented in Figure IV-C The on-board computer performs the position control of the vehicle. The ground station, running Matlab/Simulink, sets position references to be tracked and retrieves the state of the vehicle. Here, the controller presented in the paper, based on the virtual mass is implemented and used to control the platform.

A first experiments is reported in Figure 8. With reference to (20), a force f_v is assigned to the virtual mass. Due to the dynamical coupling between the vehicle and the virtual mass, the real system starts moving. At a position $p_x \approx 0.55$ m in the inertial frame, an obstacle (i.e. a wall plate) constrains the workspace of the real vehicle, causing an impact at time $t \approx 11$ s. The wall is equipped with an ATI (ATI Industrial

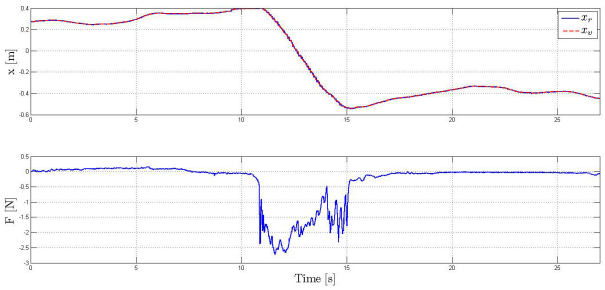

Fig. 9. The UAV is moved by the human. The virtual force applied to the virtual vehicle is set to zero. When the operator applies a force to the UAV, the overall system moves to a new equilibrium position. **Top**: the position of the UAV (continuous blue line) and of the virtual vehicle (dashed red line). **Bottom**: the force applied by the operator interacting with the UAV, measured by means of an ATI-mini40E force/torque sensor.

Automation, USA) mini40-E force/torque sensor, which is used to retrieve measurements of the interaction of the vehicle with the wall itself. More precisely, the force/torque sensor is used only to measure the interaction forces along the direction orthogonal to the wall plate, and not for control purposes.

The experiment reported here refers to a certain set of parameters of the virtual mass. Note that, as it has been shown in Section III, the proposed control strategy does not require to have access to the parameters of the real system. Both the transient and the steady state equilibrium position and, therefore, the consequent interaction forces can be modified by means of changing only the gains of the high level controller, i.e. the virtual mass parameters.

In a second experiment, the overall system is free to fly. At time $t \approx 10.5$ s the human operator introduces a force disturbance on the UAV, by pushing in the x direction. As a consequence, the quadrotor moves and it is followed by the virtual mass thus moving the entire system at hovering in a new equilibrium position. Figure 9 shows the result of the proposed controller. Also in this experiment, the force measurements are retrieved by means of a tool equipped with the ATI sensor, which is used by the human operator to apply a force on the vehicle.

V. CONCLUSIONS

The paper proposed a control strategy that allows stable and safe interaction of a generic robotic system and, more specifically, of a quadrotor UAV. The control architecture is a modified impedance controller, which is realized by means of a virtual mass. The proposed control scheme allows to qualitatively control the interaction forces arising between the robotic system and an unknown environment or a human due to contacts, without requiring the use of force measurements. The controller exploits the dynamics of the virtual mass, with the purpose of monitoring the interaction of the real system, and eventually control it by means of a force input to the virtual system.

REFERENCES

[1] K. Valavanis, Ed., *Advances in Unmanned Aerial Vehicles*. Springer, 2007.

[2] N. Michael, J. Fink, and V. Kumar, *Cooperative manipulation and transportation with aerial robots*. Autonomous Robots - Springer, 2010.

[3] A. Keemink, M. Fumagalli, S. Stramigioli, and R. Carloni, "Mechanical design of a manipulation system for unmanned aerial vehicles," in *Proceedings of the IEEE International Conference on Robotics and Automation*, 2012.

[4] Q. Lindsey, D. Mellinger, and V. Kumar, "Construction of cubic structures with quadrotor teams," in *Proceedings of Robotics: Science and Systems*, 2011.

[5] P. Pounds, D. Bersak, and A. Dollar, "Grasping from the air: Hovering capture and load stability," in *Proceedings of the IEEE International Conference on Robotics and Automation*, 2011.

[6] A. Albers, S. Trautmann, T. Howard, T. Nguyen, M. Frietsch, and C. Sauter, "Semi-autonomous flying robot for physical interaction with environment," in *Proceedings of the IEEE Conference on Robotics Automation and Mechatronics*, 2010.

[7] M. Fumagalli, R. Naldi, A. Macchelli, R. Carloni, S. Stramigioli, and L. Marconi, "Modeling and control of a flying robot for contact inspection," in *Proceedings of the IEEE/RSJ International Conference on Intelligent Robots and Systems*, 2012.

[8] J. Scholten, M. Fumagalli, S. Stramigioli, and R. Carloni, "Interaction control of an UAV endowed with a manipulator," in *Proceedings of IEEE International Conference on Robotics and Automation*, 2013.

[9] N. Diolaiti, C. Melchiorri, and S. Stramigioli, "Contact impedance estimation for robotic systems," *IEEE Transactions on Robotics*, vol. 21, no. 5, pp. 925–935, 2005.

[10] A. Isidori, *Nonlinear Control Systems II*, ser. Communication and Control Engineering Series. Springer–Verlag London, 1998.

[11] N. Hogan, "Impedance control: an approach to manipulation: parts I-III," *ASME Journal o Dynamic Systems, Measurement and Control*, vol. 107, no. 1, pp. 1–24, 1985.

[12] R. Ortega, A. van der Schaft, I. Mareels, and B. Maschke, "Putting energy back in control," *IEEE Control Systems Magazine*, vol. 21, no. 2, pp. 18–33, 2001.

[13] B. Brogliato, *Nonsmooth Mechanics Model, Dynamics and Control*. Springer, 1996.